Proceedings of the 3rd Croatian Conference on Earthquake Engineering - 3CroCEE
19–22 March 2025, Split, Croatia

DOI: https://doi.org/10.5592/CO/3CroCEE.2025.13

COMPUTED BI-DIRECTIONAL COMBINATION COEFFICIENTS FOR STRUCTURES USING THE FEB. 6TH, 2023 KAHRAMANMARAS EARTHQUAKES' GROUND MOTION DATA

Asma YAHIOAUI [(1)], Oguz KOZ [(2)], Oguz C. CELIK [(3)]

[(1)] *Ph.D., University of Sciences and Technology Houari Boumediene (USTHB), Department of Structures and Materials, Built Environmental Research Laboratory, Civil Engineering Faculty, BP 32 El Alia, Bab Ezzouar, 16111, Algiers, Algeria. email: yahiaouiasma14@gmail.com / ayahiaoui1@usthb.dz*
[(2)] *Ph.D. Student, Research Assistant, Istanbul Technical University (ITU) Faculty of Architecture, Structural & Earthquake Engineering Unit, Taskisla, Taksim, 34437, Istanbul, Turkey. email: oguz.koz@itu.edu.tr*
[(3)] *Prof, Istanbul Technical University (ITU) Faculty of Architecture, Structural & Earthquake Engineering Unit, Taskisla, – Taksim, 34437, Istanbul, Turkey. email: celikoguz@itu.edu.tr*

Abstract

The existing seismic design codes consider bi-directional effects by applying the square root sum of squares (SRSS) or the percentage rule; the latter simplified way of design is commonly employed by accounting for the 100% contribution in the assumed principal direction plus 30% or 40% other direction's contribution. Although the potential reasons of widespread building damage and collapses in the Feb. 6th, 2023 Kahramanmaras earthquake doublet have been well documented, there are still questions in mind that whether or not bi-directional effects played a significant role in this devastation. To appropriately address this, bi-directional combination coefficients can be calculated using the strong ground motion records of these earthquakes. The Housner's spectrum intensity values are calculated by using the pseudo-elastic velocity spectrum curves for both directions of the 60 records in locations where destruction was significant. Following the percentage rule, intensities both obtained from the resultant (i.e., bi-directional) and unidirectional velocity spectra are combined, and the corresponding percent values as other direction's contribution are computed. Note that pseudo-velocity spectrum curves cover a wide period range representing various types of structures and are developed for damping ratios ranging from undamped to significantly damped systems (e.g. systems with energy dissipation devices). Numerical results reveal that 50% of the selected stations from both earthquakes suggest combination coefficients in excess of the 30% rule, indicating that the 30% rule may underestimate internal forces and drifts for half of the stations. This would justify and could be one of the reasons for severe damage and collapses observed in several types of structures. Furthermore, most cases satisfied the 40% rule (this is used especially for bridges), but some exceptional cases led to higher combination coefficients, particularly those for undamped (or slightly damped) and 5% damped structures basically assumed for RC framed buildings in design codes.

1. Introduction

During an earthquake shaking, structures are highly influenced by the seismic motion characteristics [1], since they are simultaneously subjected to six ground motion components. Among them, two in the horizontal plane and one in the vertical direction are generally the most destructive for buildings [2]. Since building structures are much more flexible in lateral directions, most seismic design codes require consideration of the two horizontal orthogonal components of ground motion during the design stage. To this end, most seismic design codes allow three main methods for integrating the impact of multiple earthquake components: complete quadratic combination (CQC3), square root sum of squares (SRSS), and the percentage rule. The percentage rule, a widely accepted approach, represents the standard practice accounting for bi-directional effects by designers [3]; it consists of taking into account a 100% contribution from the earthquake's principal direction, along with a 30% or 40% contribution from the other direction. The common 100%-30% combination rule was first introduced by Rosenblueth and Contreras in 1977 [4], and then it has been adopted by the majority of building regulations, such as Eurocode 8 [5], ASCE 7-22 [6], Turkey Building Earthquake Code (TBEC-2018) [7], National Building

Proceedings of the 3rd Croatian Conference on Earthquake Engineering - 3CroCEE
19–22 March 2025, Split, Croatia

DOI: https://doi.org/10.5592/CO/3CroCEE.2025.13

Code of Canada (NBCC-2020) [8], FEMAP (2020) [9], IBC (2018) [10], GB50011-China code [11], ATC 3-06 (1978) [12], Caltrans seismic design criteria version 1.7 (2013) [13], New Zealand (2005) [14], and Iranian code (2008). The rule of 100%-40% is generally dictated by seismic codes for bridges, including ATC-32 (1996) [15] and Seismic Retrofitting Manual for Highway Structures: Part 1–Bridges (Fhwa-Hrt-06-032, 2006) [16].

On February 6th, 2023, two disastrous successive earthquakes, measuring M_w 7.8 and 7.6, struck the southwestern region of the East Anatolian Fault (EAF) [17], causing severe damage to over 2,457,942 different types of structures, including residential buildings, bridges, hospitals, and historical buildings. Note that these earthquakes claimed more than 50,000 lives as well [17]. The primary reasons for these damages were attributed to the substandard material quality of structural members since the safety and structural performance depend on it [18], in addition to the weak soil conditions. However, to date, the impact of orthogonal components has not been investigated yet. Previous studies have been conducted on analyzing various earthquakes ground motion records to predict the bi-directional impact and have concluded that the combination rules proposed by building codes are mostly conservative and sufficient [2,19]. Similar results were observed when analyzing the combination rules to predict the effects of tri-directional earthquake excitation under elastic and inelastic conditions [20–22]. To ascertain whether the combination rules suggested in existing building codes are conservative or not, this research mainly aims to revisit the bi-directional effects from the February 6th Kahramanmaras earthquakes for different structural types, from undamped to highly damped systems.

2. Dataset

From each earthquake, thirty records were downloaded from TADAS AFAD [23] based on the highest PGA values. It should be noted that the data available on AFAD are unprocessed, and using processed data would affect the results slightly. To this end, the dataset was filtered to eliminate noise-contaminated ground motion frequency content from the entire record without modifying the main ground motion characteristics in the predefined frequency band. The applied filtering process was derived from the research conducted by Jinjun Hu et al**.** [24], who investigated the characteristics of the February 6th Kahramanmaras earthquakes. Therefore, the fourth-order Butterworth noncausal filter is adopted with the high-pass and low-pass cutoff frequencies set to 0.07-30 Hz.

It should be noted that the Pazarcik earthquake records with station codes 3146, 0201, and 4632, as well as the Elbistan/Ekinozu earthquake records with station codes 4631, 0213, and 4414, were found to be of poor quality in the study corroborated by Jinjun Hu et al. [24] due to several reasons, such as the significant noise content and incorrect waveform, while Tang et al. [25] determined that the stations 4630, 4629, 4632, 2707, and 2709 were compromised and inaccurate since they sustained damage during the earthquake shaking. Therefore, these stations have been removed from the dataset. Consequently, properties of the constructed dataset to investigate the bi-directional effects of both February 6th Kahramanmaras earthquakes are presented in Table 1 and Table 2. Here, R_{JB} denotes the nearest distance to the surface projection of the fault plane, while R_{rup} indicates the closest distance to the rupture plane.

Table 1. Characteristics of the Pazarcik earthquake

Code station	Province	Longitude	Latitude	R_{JB}	R_{rup}	R_{epi}	R_{hyp}
4614	Kahramanmaras	37.297	37.485	0	8.25	31.42	32.57
3129	Hatay	36.134	36.191	75.71	75.71	146.39	146.64
3126	Hatay	36.138	36.220	72.55	72.55	143.54	143.80
3141	Hatay	36.220	36.373	54.20	54.20	125.42	125.71
3138	Hatay	36.511	36.803	9.70	9.70	71.70	72.21
3125	Hatay	36.133	36.238	70.82	70.82	142.15	142.41
NAR	Kahramanmaras	37.157	37.392	0.00	7.47	15.35	17.60
3135	Hatay	35.883	36.409	66.18	66.18	142.15	142.41
3123	Hatay	36.160	36.214	72.58	72.58	143.00	143.26

DOI: https://doi.org/10.5592/CO/3CroCEE.2025.13

2718	Gaziantep	36.627	37.008	0.00	2.10	48.30	49.06
3142	Hatay	36.366	36.498	38.09	38.09	106.49	106.84
3144	Hatay	36.486	36.757	12.36	12.36	77.04	77.52
4616	Kahramanmaras	36.838	37.375	14.03	22.42	20.54	22.27
3145	Hatay	36.406	36.645	21.68	21.68	91.13	91.54
4615	Kahramanmaras	37.138	37.387	0.00	8.02	13.83	16.28
3139	Hatay	36.414	36.584	28.54	28.54	96.19	96.57
3124	Hatay	36.172	36.239	69.66	69.66	140.11	140.37
2712	Gaziantep	36.733	37.184	2.74	11.58	29.79	31.01
3136	Hatay	36.247	36.116	81.47	81.47	148.38	148.63
3132	Hatay	36.172	36.207	73.08	73.08	143.12	143.38
4625	Kahramanmaras	36.982	37.539	20.83	28.96	28.40	29.67
3137	Hatay	36.489	36.693	18.44	18.44	82.48	82.93
3143	Hatay	36.557	36.849	8.10	8.10	65.13	65.70
4621	Kahramanmaras	36.929	37.593	28.49	36.32	35.42	36.45
3131	Hatay	36.163	36.191	74.95	74.95	144.98	145.23
4624	Kahramanmaras	36.918	37.536	24.02	32.02	29.73	30.95
4611	Kahramanmaras	37.284	37.747	23.28	31.32	55.32	55.98

Table 2. Characteristics of the Elbistan/Ekinozu earthquake

Code station	Province	Longitude	Latitude	R_{JB}	R_{rup}	R_{epi}	R_{hyp}
4612	Kahramanmaras	36.482	38.024	62.18	62.18	66.68	67.05
4406	Malatya	37.974	38.344	60.69	66.64	70.17	70.52
4409	Malatya	37.491	38.561	19.26	27.02	56.86	57.28
3802	Kayseri	36.504	38.478	58.12	58.12	77.41	77.73
4611	Kahramanmaras	37.284	37.747	0.00	6.85	38.21	38.85
4614	Kahramanmaras	37.298	37.485	0.95	7.09	67.35	67.71
4412	Malatya	38.184	38.597	79.75	84.86	99.89	100.14
4405	Malatya	37.940	38.811	60.32	66.23	100.81	101.05
0129	Adana	36.211	38.259	84.76	84.76	91.84	92.11
NAR	Kahramanmaras	37.157	37.392	12.13	10.85	77.85	78.16
4410	Malatya	37.679	38.867	41.23	47.57	94.59	94.84
2703	Gaziantep	37.350	37.058	48.50	49.49	115.06	115.27
5807	Sivas	37.248	38.727	4.52	8.65	70.94	71.28
4613	Kahramanmaras	36.357	37.570	75.34	75.34	96.56	96.82
0130	Adana	35.671	37.252	139.26	21.83	166.46	166.61
4625	Kahramanmaras	36.982	37.539	20.34	20.34	65.22	65.60
0125	Adana	35.796	37.015	136.49	60.84	174.48	174.62
2308	Elazig	39.310	38.451	177.65	180.07	185.23	185.36
4620	Kahramanmaras	36.898	37.586	27.51	27.51	63.46	63.84
8002	Osmaniye	36.562	37.192	66.70	33.24	116.24	116.45
4624	Kahramanmaras	36.918	37.536	26.03	26.03	67.65	68.01
2309	Elazig	38.727	38.799	127.82	131.16	151.77	151.93
3144	Hatay	36.486	36.757	104.09	78.92	162.37	162.52
5809	Sivas	37.382	39.231	61.28	63.39	127.57	127.76
4616	Kahramanmaras	36.838	37.375	35.67	11.62	86.81	87.09
0127	Adana	35.920	37.816	112.56	112.56	119.52	119.73
4617	Kahramanmaras	36.830	37.586	33.53	33.53	66.50	66.87

3. Methodology

After preprocessing the data, the Newmark-beta method [26] for linear systems is employed to compute the elastic response spectrum, namely the velocity spectrum and the pseudo velocity. Therefore, computing the Housner intensity (SI), which best assesses the damage potential of an earthquake [27], is as follows:

$$SI = \int_{0.1}^{2.5} PS_v(\varepsilon, T, dt)dT \quad \text{Eq. 1}$$

Proceedings of the 3rd Croatian Conference on Earthquake Engineering - 3CroCEE
19–22 March 2025, Split, Croatia

DOI: https://doi.org/10.5592/CO/3CroCEE.2025.13

Where PS_v represents the pseudo velocity, T is the fundamental period of a single degree e of freedom system (representing the real building) and ζ is the damping ratio.

In this numerical work, four values of damping ratio (0%, 5%, 20%, and 50%) are considered to demonstrate the impact of damping ratio on various structures ranging from undamped systems to significantly damped systems. Additionally, as explained before, it is known that building codes typically incorporate bi-directional effects through the application of combination rules of 30% or 40%, signifying the total contribution of the principal direction of the earthquake, along with a 30% or 40% contribution from the other direction. These combination rules can be expressed as follows:

$$E_{XY} = E_X + \lambda_1 E_y \quad \text{Eq. 2}$$

$$E_{XY} = \lambda_2 E_x + E_y \quad \text{Eq. 3}$$

Here, λ_1 and λ_2 represent the percentage of the contribution in the other earthquake direction, when two orthogonal records are taken into account. However, combination coefficients proposed in building codes, such as 30% or 40%, are generally calculated based on the principal direction's acceleration record. This study revisits the bi-directional effects using the February 6th Kahramanmaras earthquakes, considering the contributions of other components. Consequently, the α coefficient, as introduced below, is particularly significant for assessing the combination rules in structural codes, and it is expressed as follows:

$$E_{xy} = E_x + \alpha E_x \quad \text{Eq. 4}$$

From the equations given above, λ_1, λ_2, and α can be calculated as follows:

$$\lambda_1 = (SI^{xy} - SI^x)/SI^y \quad \text{Eq. 5}$$

$$\lambda_2 = (SI^{xy} - SI^y)/SI^x \quad \text{Eq. 6}$$

$$\alpha = \frac{SI^{xy}}{SI^x} - 1 \quad \text{Eq. 7}$$

In which x denotes the earthquake's major direction that produces the maximum internal forces. Also, SI^x, SI^y, and SI^{xy} represent the Housner intensities to be calculated for both orthogonal directions and for the resultant alone.

The procedure for obtaining the spectral intensities for each earthquake component and the resultant accounting for the contribution of the two orthogonal directions of the earthquake is illustrated in Figure 1. The methodology to be followed in this work is summarized in Figure 2 in the form of a flowchart.

Proceedings of the 3rd Croatian Conference on Earthquake Engineering - 3CroCEE
19–22 March 2025, Split, Croatia

DOI: https://doi.org/10.5592/CO/3CroCEE.2025.13

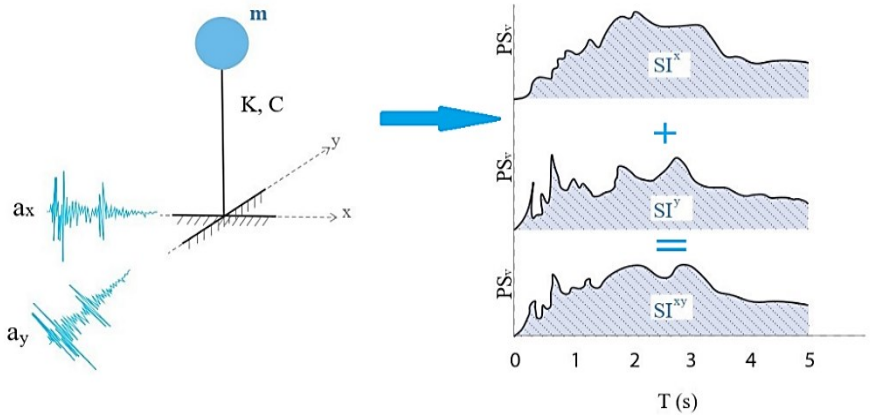

Figure 1. Typical SDOF system subjected to bi-directional seismic excitations and calculated spectral intensities

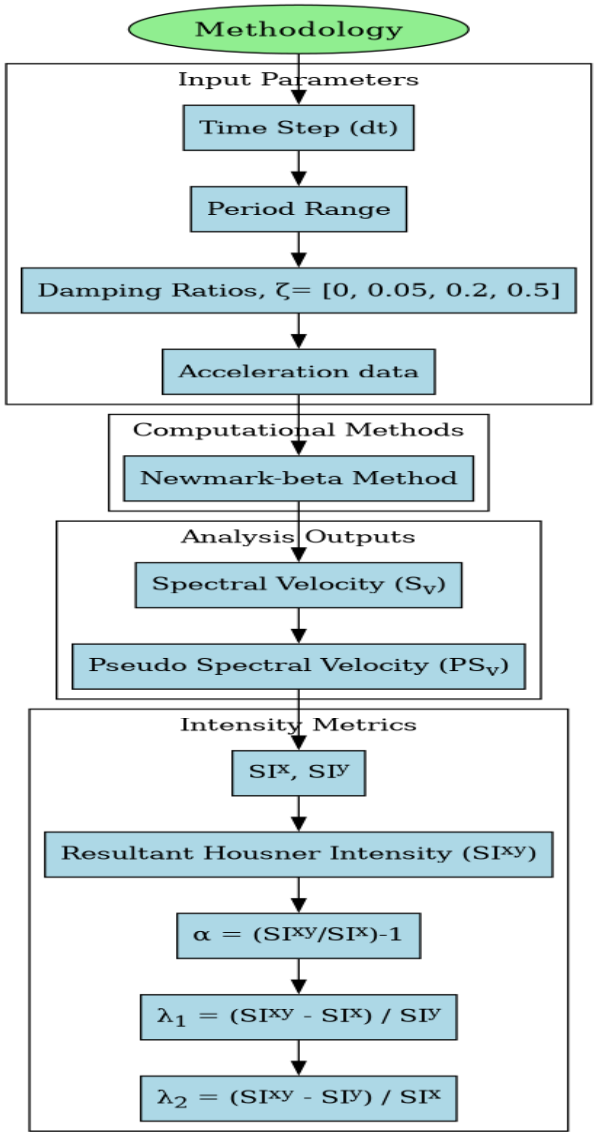

Figure 2. Flowchart of methodology to be followed

Proceedings of the 3rd Croatian Conference on Earthquake Engineering - 3CroCEE
19–22 March 2025, Split, Croatia

DOI: https://doi.org/10.5592/CO/3CroCEE.2025.13

4. Numerical Results and Discussion

4.1. Combination Coefficients for the Feb. 6th, Kahramanmaras (Pazarcik) EQ (M_w 7.8)

Analysis results from the 27 stations selected from the Pazarcik earthquake are illustrated in Table 3. It is clear that nine records for all damping values exhibit α values exceeding 0.3, as suggested by many seismic codes. This data set represents one-third of the total records. For undamped systems, 20 stations surpassed 0.3, while nine stations exceeded 0.4. Moreover, for the damping ratio of 0.05, mainly used for residential RC framed buildings, 14 stations surpassed 0.3, representing over half of the total records, while six records exceeded the value of 0.4. For a damping ratio equal to 20%, the α value surpassed 0.3 in 13 stations, while four records reached or exceeded 0.4. In 11 records, the α values were greater than 0.3, with three stations showing values exceeding 0.4 when the damping ratio is 50%. Therefore, the lower and upper bounds of α for ζ = 0, 0.05, 0.20, and 0.50 are obtained to be 0.20~0.44, 0.14~0.42, 0.16~0.44, and 0.13~0.40, respectively.

Table 3. Computed Housner Intensities and combination coefficients for the February 6th, Kahramanmaras (Pazarcik) earthquake

Stations		ζ = 0%				5%				20%				50%			
		SI (cm/s)	α	λ1	λ2	SI (cm/s)	α	λ1	λ2	SI (cm/s)	α	λ1	λ2	SI (cm/s)	α	λ1	λ2
4614	EW	435.02				162.21				92.38				58.15			
	NS	511.60	**0.34**	0.40	0.49	205.03	0.28	0.35	0.49	120.76	0.26	0.34	0.50	76.81	0.26	0.34	0.50
	R	687.44				262.61				152.38				96.50			
3129	EW	570.06				284.00				166.97				104.98			
	NS	918.08	0.21	0.33	0.58	548.84	0.14	0.28	0.62	334.04	0.13	0.25	0.63	194.70	0.14	0.26	0.60
	R	1106.89				627.00				376.56				221.65			
3126	EW	583.27				268.24				159.48				90.66			
	NS	710.79	**0.32**	0.39	0.50	380.47	0.25	0.35	0.54	222.70	0.24	0.34	0.53	135.13	0.21	0.31	0.54
	R	937.92				474.38				276.73				163.09			
3141	EW	741.73				396.86				236.84				141.89			
	NS	565.88	0.30	0.39	0.54	293.29	0.26	0.36	0.52	164.33	0.23	0.33	0.53	97.19	0.22	0.33	0.54
	R	963.62				501.01				290.78				173.50			
3138	EW	743.78				501.13				314.91				200.18			
	NS	730.49	**0.44**	0.45	0.46	482.27	**0.42**	0.44	0.46	307.89	**0.44**	0.44	0.46	187.82	**0.40**	0.43	0.47
	R	1071.16				713.86				451.90				281.02			
3125	EW	561.39				272.95				164.95				98.40			
	NS	446.59	**0.31**	0.39	0.51	231.51	**0.32**	0.38	0.47	139.74	**0.31**	0.37	0.47	87.90	**0.34**	0.39	0.45
	R	735.50				360.72				216.85				132.29			
NAR	EW	379.10				221.59				147.81				92.44			
	NS	350.79	**0.39**	0.42	0.46	205.17	**0.37**	0.40	0.45	145.09	**0.41**	0.42	0.43	95.97	**0.39**	0.41	0.43
	R	525.19				304.45				208.63				133.45			
3135	EW	400.06				231.25				153.90				91.66			
	NS	326.39	**0.31**	0.38	0.50	181.20	0.28	0.35	0.49	120.62	0.27	0.35	0.49	85.67	**0.37**	0.40	0.44
	R	524.59				294.97				195.83				125.86			
3123	EW	749.90				407.40				212.27				118.32			
	NS	1001.11	0.29	0.38	0.54	581.76	0.25	0.35	0.54	372.74	0.17	0.29	0.60	228.00	0.13	0.26	0.61
	R	1288.69				724.33				434.32				258.24			
2718	EW	419.13				249.33				151.14				105.31			
	NS	352.43	**0.38**	0.45	0.53	210.14	**0.35**	0.42	0.51	125.75	**0.32**	0.39	0.49	74.17	0.23	0.33	0.53
	R	576.49				337.42				199.64				129.99			
3142	EW	385.79				203.70				120.57				70.82			
	NS	375.38	**0.42**	0.43	0.44	212.21	**0.40**	0.42	0.44	140.15	**0.32**	0.38	0.46	90.35	0.27	0.35	0.49
	R	546.43				296.89				185.62				115.19			
3144	EW	442.38	**0.41**	0.43	0.45	260.84	**0.40**	0.42	0.44	166.88	**0.42**	0.42	0.42	101.32	**0.40**	0.41	0.42
	NS	457.38				272.74				166.76				103.92			

Proceedings of the 3rd Croatian Conference on Earthquake Engineering - 3CroCEE
19–22 March 2025, Split, Croatia

DOI: https://doi.org/10.5592/CO/3CroCEE.2025.13

	R	646.40				381.99				237.43				145.38			
	EW	370.63				199.87				110.70				66.04			
4616	NS	420.58	**0.36**	0.41	0.48	220.94	**0.37**	0.40	0.46	158.56	0.22	0.32	0.53	116.56	0.15	0.27	0.58
	R	573.79				301.79				193.99				134.10			
	EW	631.89				410.98				247.41				153.52			
3145	NS	371.84	0.20	0.33	0.61	241.90	0.17	0.30	0.59	151.80	0.18	0.29	0.56	102.84	0.21	0.31	0.54
	R	755.14				482.71				290.98				185.12			
	EW	640.93				315.70				211.22				122.72			
4615	NS	491.27	0.29	0.38	0.52	244.92	0.29	0.37	0.51	163.13	0.27	0.35	0.50	102.52	**0.31**	0.37	0.47
	R	825.79				406.90				268.21				160.22			
	EW	854.12				465.26				232.57				140.29			
3139	NS	803.17	**0.41**	0.43	0.47	517.95	**0.35**	0.39	0.46	323.59	0.23	0.32	0.51	195.07	0.23	0.32	0.51
	R	1201.24				701.28				398.74				240.44			

Table 4 (Continued). Computed Housner Intensities and combination coefficients for the February 6th, Kahramanmaras (Pazarcik) earthquake

Stations		**ζ = 0%**				**5%**				**20%**				**50%**			
		SI (cm/s)	α	λ1	λ2	SI (cm/s)	α	λ1	λ2	SI (cm/s)	α	λ1	λ2	SI (cm/s)	α	λ1	λ2
	EW	710.58				387.95				219.68				128.70			
3124	NS	774.30	**0.41**	0.45	0.49	450.88	**0.37**	0.43	0.51	259.03	**0.33**	0.39	0.49	160.13	0.29	0.36	0.49
	R	1092.11				617.56				345.31				206.62			
	EW	563.42				325.46				215.48				136.20			
2712	NS	380.29	0.23	0.34	0.56	190.83	0.17	0.29	0.58	125.07	0.16	0.27	0.58	91.83	0.21	0.31	0.53
	R	694.38				380.34				249.81				164.33			
	EW	333.28				151.48				81.02				46.96			
3136	NS	406.73	**0.32**	0.40	0.51	211.38	0.24	0.34	0.53	124.90	0.20	0.30	0.55	74.29	0.19	0.30	0.56
	R	538.87				262.90				149.45				88.49			
	EW	412.83				222.60				135.21				77.21			
3132	NS	518.46	**0.32**	0.40	0.52	291.83	0.28	0.37	0.52	173.66	0.28	0.36	0.50	103.62	0.25	0.34	0.51
	R	682.50				374.13				221.68				129.59			
	EW	440.77				177.18				99.38				60.36			
4625	NS	470.78	**0.40**	0.43	0.47	230.17	0.28	0.36	0.51	144.52	0.22	0.33	0.54	95.76	0.19	0.29	0.55
	R	660.18				293.66				176.86				113.48			
	EW	421.42				228.26				133.48				82.68			
3137	NS	388.17	**0.38**	0.41	0.46	209.77	**0.36**	0.40	0.45	115.03	**0.33**	0.38	0.47	72.07	**0.33**	0.38	0.46
	R	582.06				311.50				177.70				110.06			
	EW	403.11				249.73				157.18				96.95			
3143	NS	425.52	**0.41**	0.43	0.46	277.83	**0.35**	0.39	0.46	163.36	**0.40**	0.41	0.44	93.97	**0.40**	0.41	0.43
	R	598.89				376.44				228.32				135.41			
	EW	343.99				150.87				75.82				44.65			
4621	NS	352.11	**0.43**	0.44	0.45	145.42	**0.40**	0.41	0.43	80.01	**0.39**	0.41	0.44	50.63	**0.35**	0.39	0.46
	R	503.10				210.96				111.06				68.18			
	EW	375.73				222.63				128.90				75.74			
3131	NS	272.20	0.27	0.37	0.54	168.84	0.27	0.35	0.51	109.90	**0.32**	0.38	0.47	65.28	**0.33**	0.38	0.47
	R	476.33				282.39				170.62				100.59			
	EW	488.22				202.23				115.95				71.69			
4624	NS	439.02	**0.37**	0.41	0.47	196.92	**0.41**	0.42	0.44	122.58	**0.38**	0.40	0.43	87.57	0.29	0.36	0.47
	R	669.91				285.08				169.21				113.27			
	EW	242.72				121.07				71.43				41.76			
4611	NS	253.15	**0.42**	0.43	0.46	116.98	**0.40**	0.42	0.44	62.78	**0.33**	0.38	0.46	35.67	**0.32**	0.37	0.46
	R	358.24				169.88				95.33				54.99			

Proceedings of the 3rd Croatian Conference on Earthquake Engineering - 3CroCEE
19–22 March 2025, Split, Croatia

DOI: https://doi.org/10.5592/CO/3CroCEE.2025.13

4.2.Combination Coefficients for the Feb. 6th, Kahramanmaras (Elbistan/Ekinozu) EQ (M_w 7.6)

Similarly, analysis results from the 27 stations selected from the Elbistan/Ekinozu earthquake are presented in Table 5; it is observed that 11 records across all damping values exhibit α values exceeding 0.3, accounting for 41% of the total records. For 26 stations, the α value surpassed 0.3 for undamped systems, while in 10 stations, it exceeded 0.4. As for the remaining 16 records and for residential RC framed buildings having a damping value of 0.05, α values surpassed 0.3, representing nearly 60% of the records, and four records exceeded or equaled to 0.4. For damping ratios equal to 20% and 50%, the α value exceeded 0.3 in 12 records and in nine stations, respectively. Consequently, the lower and upper bounds of α for ζ = 0, 0.05, 0.20, and 0.50 are obtained to be 0.27~0.46, 0.22~0.42, 0.18~0.39, and 0.14~0.40, respectively.

Table 5. Computed Housner Intensities and combination coefficients for the February 6th, Kahramanmaras (Elbistan/Ekinozu) earthquake

Stations		ζ = 0%				5%				20%				50%			
		SI (cm/s)	α	λ1	λ2	SI (cm/s)	α	λ1	λ2	SI (cm/s)	α	λ1	λ2	SI (cm/s)	α	λ1	λ2
4612	EW	524.88	**0.32**	0.38	0.49	313.02	0.26	0.35	0.50	174.49	0.18	0.29	0.56	100.49	0.14	0.26	0.59
	NS	630.41				409.58				280.92				183.22			
	R	830.97				517.69				330.96				209.10			
4406	EW	210.55	**0.40**	0.42	0.45	97.95	**0.39**	0.41	0.44	51.04	**0.39**	0.41	0.43	28.82	**0.36**	0.39	0.44
	NS	221.70				92.93				48.77				31.17			
	R	310.78				135.68				70.87				42.48			
4409	EW	94.83	**0.35**	0.41	0.50	45.08	0.27	0.36	0.53	23.15	0.29	0.37	0.50	14.50	0.30	0.36	0.47
	NS	80.62				33.38				18.43				11.93			
	R	127.93				57.20				29.96				18.81			
3802	EW	342.44	**0.39**	0.44	0.51	137.37	**0.32**	0.39	0.50	77.06	0.24	0.34	0.53	44.66	0.24	0.33	0.51
	NS	301.11				113.22				54.69				32.99			
	R	475.13				181.75				95.40				55.57			
4611	EW	169.77	0.27	0.38	0.55	75.41	0.22	0.32	0.55	42.46	0.24	0.33	0.53	25.74	0.22	0.32	0.53
	NS	122.51				50.22				30.17				17.84			
	R	215.88				91.70				52.52				31.52			
4614	EW	75.02	**0.42**	0.43	0.46	34.60	0.25	0.34	0.51	22.00	0.23	0.33	0.53	17.16	0.18	0.29	0.58
	NS	72.13				25.67				15.37				10.28			
	R	106.24				43.38				27.03				20.17			
4412	EW	209.54	**0.43**	0.44	0.45	93.58	**0.37**	0.41	0.45	53.48	**0.38**	0.41	0.46	37.92	**0.33**	0.38	0.47
	NS	214.79				101.88				57.73				32.73			
	R	306.45				139.91				79.78				50.40			
4405	EW	78.32	**0.46**	0.46	0.46	33.16	**0.42**	0.44	0.46	17.14	**0.37**	0.41	0.46	10.11	**0.38**	0.41	0.44
	NS	79.04				34.58				18.72				10.71			
	R	115.02				49.19				25.67				14.81			
129	EW	58.99	**0.41**	0.43	0.45	25.03	**0.36**	0.39	0.44	15.22	**0.39**	0.41	0.43	11.12	**0.31**	0.37	0.46
	NS	61.13				27.25				15.76				9.49			
	R	86.40				37.11				21.94				14.63			
NAR	EW	46.76	**0.35**	0.41	0.49	21.77	0.29	0.36	0.49	14.82	0.24	0.34	0.52	11.62	0.20	0.31	0.55
	NS	40.29				17.46				10.82				7.59			
	R	63.32				28.09				18.45				13.97			
4410	EW	102.01	**0.46**	0.46	0.47	48.41	**0.36**	0.41	0.47	28.42	**0.33**	0.38	0.46	16.37	**0.37**	0.40	0.44
	NS	100.95				43.05				24.66				15.20			
	R	148.52				65.90				37.71				22.37			
2703	EW	97.19	**0.35**	0.41	0.50	39.68	0.29	0.37	0.50	20.73	**0.34**	0.39	0.46	13.45	0.30	0.36	0.47
	NS	82.57				31.43				18.28				11.14			
	R	130.80				51.26				27.80				17.50			

Proceedings of the 3rd Croatian Conference on Earthquake Engineering - 3CroCEE
19–22 March 2025, Split, Croatia

DOI: https://doi.org/10.5592/CO/3CroCEE.2025.13

5807	EW	96.52	**0.34**	0.41	0.49	45.23	0.25	0.34	0.51	25.26	0.24	0.33	0.51	14.02	0.30	0.37	0.47
	NS	82.12				33.16				18.59				11.66			
	R	129.81				56.44				31.45				18.29			
4613	EW	67.85	**0.44**	0.45	0.47	32.97	**0.42**	0.42	0.43	17.98	**0.36**	0.39	0.45	12.14	**0.35**	0.39	0.44
	NS	65.68				32.44				19.71				13.32			
	R	97.54				46.73				26.79				18.04			
0130	EW	148.11	**0.42**	0.43	0.46	65.46	**0.37**	0.40	0.44	38.77	**0.35**	0.39	0.45	24.84	**0.38**	0.40	0.43
	NS	154.12				69.79				43.08				26.06			
	R	218.41				95.94				58.03				36.06			
4625	EW	112.26	**0.33**	0.39	0.49	42.87	**0.31**	0.37	0.47	21.07	0.26	0.34	0.50	12.71	0.24	0.33	0.51
	NS	134.51				51.03				27.93				17.39			
	R	178.50				66.84				35.06				21.55			

Table 6 (Continued). Computed Housner Intensities and combination coefficients for the February 6th, Kahramanmaras (Elbistan/Ekinozu) earthquake

Stations		**ζ = 0%**				**5%**				**20%**				**50%**			
		SI (cm/s)	α	λ1	λ2	SI (cm/s)	α	λ1	λ2	SI (cm/s)	α	λ1	λ2	SI (cm/s)	α	λ1	λ2
0125	EW	192.32	**0.33**	0.40	0.50	78.43	**0.32**	0.37	0.47	40.94	**0.30**	0.36	0.47	25.63	**0.30**	0.36	0.47
	NS	228.93				92.00				49.36				30.70			
	R	306.57				121.21				64.14				40.00			
2308	EW	122.55	**0.39**	0.42	0.46	57.55	**0.42**	0.42	0.42	31.25	**0.38**	0.40	0.44	16.81	**0.31**	0.37	0.47
	NS	113.47				57.06				33.11				19.84			
	R	169.88				81.44				45.72				26.07			
4620	EW	118.05	**0.37**	0.42	0.50	61.26	**0.31**	0.39	0.50	39.72	0.24	0.34	0.52	25.39	0.27	0.35	0.50
	NS	101.96				49.72				28.44				19.37			
	R	161.38				80.52				49.28				32.09			
8002	EW	57.42	**0.37**	0.43	0.50	23.47	**0.33**	0.40	0.51	12.44	**0.37**	0.42	0.48	7.15	**0.39**	0.42	0.46
	NS	65.88				28.58				14.02				7.64			
	R	90.54				37.99				19.19				10.63			
4624	EW	137.18	**0.32**	0.39	0.49	50.85	0.28	0.35	0.49	27.05	0.28	0.36	0.40	16.49	**0.31**	0.37	0.47
	NS	165.27				64.80				33.79				19.63			
	R	218.21				82.64				43.40				25.72			
2309	EW	26.78	**0.42**	0.44	0.47	9.63	**0.40**	0.42	0.45	4.88	**0.34**	0.38	0.46	3.04	0.28	0.35	0.48
	NS	25.52				9.19				5.56				3.81			
	R	38.10				13.48				7.43				4.87			
3144	EW	66.38	**0.32**	0.38	0.49	29.27	0.29	0.36	0.48	17.24	0.29	0.36	0.48	10.82	0.29	0.36	0.49
	NS	55.27				23.62				13.84				8.69			
	R	87.54				37.79				22.20				13.97			
5809	EW	133.96	**0.38**	0.43	0.50	44.24	**0.34**	0.39	0.47	21.91	**0.35**	0.39	0.45	14.34	**0.36**	0.39	0.44
	NS	118.10				38.83				19.75				13.10			
	R	184.59				59.50				29.59				19.43			
4616	EW	42.77	**0.44**	0.45	0.45	17.72	**0.36**	0.39	0.44	11.89	0.28	0.35	0.49	8.51	0.23	0.33	0.52
	NS	42.95				16.27				9.32				6.04			
	R	62.04				24.15				15.18				10.49			
0127	EW	54.77	**0.34**	0.40	0.49	27.11	0.27	0.35	0.50	15.64	0.27	0.35	0.49	9.94	**0.40**	0.41	0.42
	NS	46.36				20.88				12.21				9.77			
	R	73.15				34.38				19.86				13.95			
4617	EW	155.50	**0.34**	0.41	0.50	76.21	0.29	0.37	0.50	46.44	0.26	0.34	0.50	32.11	0.25	0.33	0.50
	NS	130.91				60.28				35.41				24.11			
	R	208.78				98.47				58.56				40.16			

DOI: https://doi.org/10.5592/CO/3CroCEE.2025.13

4.3. Analysis of earthquake damage

The Ministry of Environment, Urbanization, and Climate Change [28,29] reported that Hatay experienced the most extensive destruction, with nearly 20% of 406,849 buildings either collapsed, necessitating urgent demolition, or severely damaged, while approximately 31% sustained so-called slight to moderate damage. Note that no detailed scoring for this classification is available. Notably, of the 27 selected stations for the Pazarcik earthquake based on the highest PGA, seventeen are located in Hatay, while 18 stations from both earthquakes are situated in the province of Kahramanmaras. Table 3, Table 5, and Figure 3 indicate that one-third of the selected stations from the Pazarcik earthquake exhibited an α coefficient exceeding 0.3 across all damping values; six of these stations are located in Hatay, while the others are in Kahramanmaras. The same finding was reached for the Elbistan/Ekinozu Earthquake, wherein the majority of the α coefficient over 0.3 was seen in Kahramanmaras and Malatya. Consequently, it is determined that, alongside soil liquefaction and poor-quality concrete strength [17], the bi-directional impact has also been a contributing factor to the extensive damage sustained during the February 6th, 2023 Kahramanmaras earthquakes.

Note that most stations in the Pazarcik Earthquake are in regions of high seismic hazard, while in the Elbistan/Ekinozu earthquake, some of the stations are located in regions with low to moderate seismic hazard. It is concluded that the damage distribution in the earthquake hit region mostly matched well with the locations of larger computed bidirectional coefficients (Figure 3).

a) The Pazarcik Earthquake

b) The Elbistan/Ekinozu Earthquake

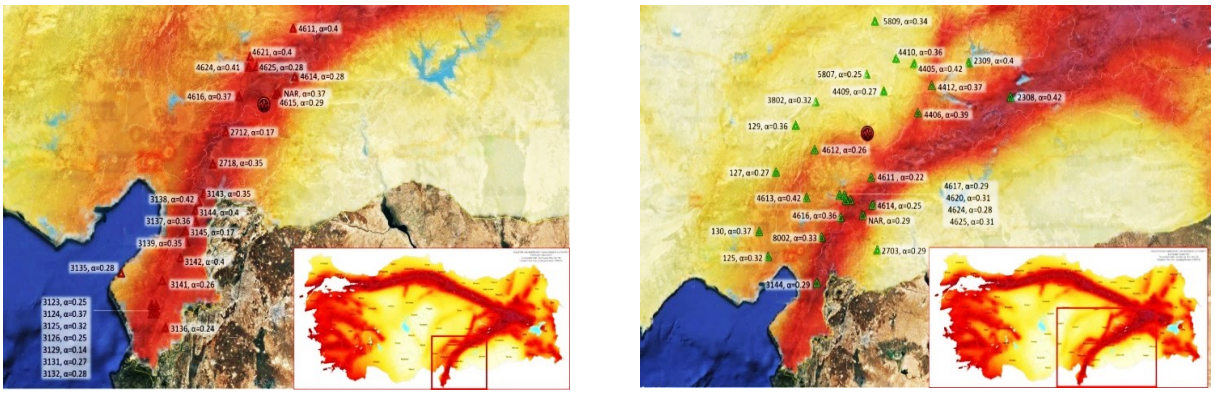

Figure 3. Distribution of α over selected stations for both earthquakes [30]

5. Conclusions

The bi-directional effects of earthquakes on buildings have been revisited. Since building damage is better reflected by the Housner Spectrum Intensity (SI) values of recorded strong ground motions, SI values in X, Y, and XY directions have been numerically computed by using the latest 2023 Kahramanmaras earthquake sequence. To derive the velocity and subsequently, pseudo velocity, the Newmark-beta approach has been followed in computing the Housner intensity. The widely used combination coefficient (i.e., α as introduced in the text) has been computed for different structural types (various damping ratios and fundamental periods). Numerical calculations reveal that one-third of the chosen stations for both earthquakes led to the α coefficients over 0.3. In addition, over half of the stations with damping values set to 5% had contributions from the other orthogonal direction above 30%, justifying the major destructions in residential buildings, while the 40% rule was satisfied in most cases.

It is important to highlight that, for both Pazarcik and Elbistan/Ekinozu earthquakes, the highest α coefficients for undamped systems were obtained to be 0.44 and 0.46, respectively. This value has been obtained to be 0.42 for both earthquakes for damping values equal to 5%, while it reached 0.44 and 0.39, respectively, for damping ratio equal to 20%. For highly damped structures (e.g. systems with

DOI: https://doi.org/10.5592/CO/3CroCEE.2025.13

seismic energy dissipators of any kind), this α coefficient attained 0.40 for both earthquakes. These highest α coefficients reflect the importance of bi-directional effects during the Kahramanmaras earthquakes. Buildings located in Hatay/Antioch, Kahramanmaras, and Malatya were mostly affected from bidirectional effects. Therefore, in addition to other structural and geotechnical problems, it could be concluded that one of the reasons for the widespread damage and collapses was bidirectional effects of the strong ground motion.

Although some exceptions were noticed, it seems that the rule of 40% would be more appropriate for such strong events for most of the structural types. Based on these computed values, it would be judgeable to relate combination coefficients to the building importance factor (i.e., return period). Moreover, some stations that exhibited high PGA values during the Elbistan/Ekinozu earthquake are located in the existing seismic hazard maps with low to moderate seismicity, yielding misleading results in the computation of the seismic forces and corresponding seismic demands during the design stage.

References

[1] Yahiaoui A, Dorbani S, Yahiaoui L. Machine learning techniques to predict the fundamental period of infilled reinforced concrete frame buildings. Structures 2023;54. https://doi.org/10.1016/j.istruc.2023.05.052.

[2] Khaled A, Tremblay R, Massicotte B. Effectiveness of the 30%-rule at predicting the elastic seismic demand on bridge columns subjected to bi-directional earthquake motions. Eng Struct 2011;33:2357–70.

[3] Wang J, Burton H V., Dai K. Combination Rules Used to Account for Orthogonal Seismic Effects: State-of-the-Art Review. J Struct Eng 2019;145:03119001.

[4] Rosenblueth, E., & Contreras H. Approximate design for multicomponent earthquakes. J Eng Mech Div 1977;103:881–93.

[5] Eurocode8. Eurocode 8 : Design of Structures for Earthquake Resistance—Part 1: General Rules. Seismic Actions and Rules for Buildings. 2004.

[6] ASCE. ASCE/SEI 7-16 Minimum Design Loads and Associated Criteria for Buildings and Other Structures. American Society of Civil Engineers; 2017.

[7] TBEC 2018: Turkish Building Earthquake Code 2018:416.

[8] National Building Code of Canada Volume 1. Natl Res Counc Canada 2020.

[9] NEHRP Recommended seismic provisions for new buildings and other structures (FEMAP 2082-1) 2020.

[10] International Code Council. International Building Code (IBC). 2018.

[11] Code for Seismic Design of Buildings (GB 50011-2010) 2010:1–171.

[12] ATC3-06. Applied Technology Council Associated with the Structural Engineers Association of Califorina 1978.

[13] seismic design criteria Version 1.7. Caltrans 2013.

[14] NZS 1170.5. Structural Design Actions Part 5: Earthquake actions – New Zealand. 2004.

[15] Applied Technology Council ATC32. Improved seismic design criteria for California bridges: Provisional recommendations. 1996.

[16] Seismic Retrofitting Manual for Highway Structures : Part 1 – Bridges. Fhwa-Hrt-06-032 2006:658.

[17] Celik OC, Ulker MBC, Gocer C, Guntepe S, Koz O, Eyupgiller MM, et al. Multidisciplinary reconnaissance investigation covering structural, geotechnical, and architectural based damage to mid-rise residential buildings following the February 6th, 2023 Kahramanmaraş, Türkiye earthquake doublets (Mw 7.8, Mw 7.6). Soil Dyn Earthq Eng 2024;182:108738.

[18] Yahiaoui A, Matos J., Dorbani S. Probabilistic forecast of concrete compressive strength using ML. 20th Int. Probabilistic Work. IPW 2024. Cham : Spr, Cham : Springer Nature Switzerland; 2024, p. 281–6. https://doi.org/https://doi.org/10.1007/978-3-031-60271-9_25.

DOI: https://doi.org/10.5592/CO/3CroCEE.2025.13

[19] Sesigur H, Celik OC, Cili F. Review and Evaluation of Combination Rules for Structures under Bi-directional Earthquake Excitations. 13th World Conf Earthq Eng 2004.

[20] Sesigur H, Celik OC, Cili F. Analysis of Code-Defined Combination Rules under Tri-Directional Earthquake Excitation. ECCOMAS Themat Conf Comput Methods Struct Dyn Earthq Eng 2007:13–6.

[21] Sesigur H, Celik OC, Cili F. Determination of orthogonal combination coefficients using inelastic velocity response spectra. ECCOMAS Themat. Conf. Comput. Methods Struct. Dyn. Earthq. Eng., 2009.

[22] Sesigur H, Celik OC, Cili F. Combination coefficients for yielding structures under tri-directional earthquake excitations. ECCOMAS Themat. Conf. Comput. Methods Struct. Dyn. Earthq. Eng., 2011.

[23] AFAD - TADAS n.d. https://tadas.afad.gov.tr/map (accessed December 3, 2024).

[24] Hu J, Liu M, Taymaz T, Ding L, Irmak TS. Characteristics of strong ground motion from the 2023 Mw 7.8 and Mw 7.6 Kahramanmaraş earthquake sequence. Bull Earthq Eng 2023:1–30.

[25] Tang Y, Şeşetyan K, Mai PM. Comprehensive ground-motion characterization of the 6 February 2023 MW 7.8 Pazarcık earthquake in Kahramanmaraş, Türkiye: insights into attenuation effects, site responses and source properties. Bull Earthq Eng 2024;22:6829–57.

[26] Newmark NM. A method of computation for structural dynamics. J Eng Mech Div 1959;85:67–94.

[27] Hussain N, Alam MS, Aman M. Seismic design coefficients verification of regular and vertically irregular high-rise shear wall buildings using bidirectional horizontal ground motions and 3D modeling. Structures 2024;70:107835.

[28] Ministry of Environment Urbanization and Climate Change, Damage Assessment Enquiry 2024. http://hasartespit.csb.gov.tr/ (accessed December 4, 2024).

[29] Damcı E, Temür R, Kanbir Z, Şekerci Ç, Köroğlu EÖ. Comprehensive investigation of damage due to 2023 Kahramanmaraş Earthquakes in Türkiye: Causes, consequences, and mitigation. J Build Eng 2024;99:111420. https://doi.org/https://doi.org/10.1016/j.jobe.2024.111420.

[30] Türkiye Deprem Tehlike Haritası n.d. https://www.afad.gov.tr/turkiye-deprem-tehlike-haritasi (accessed December 4, 2024).